Colloid Polym Sci 278: 1061–1069 (2000)

ORIGINAL CONTRIBUTION

C. Wutz
N. Stribeck
D. Gieseler

Investigation of molecular order and phase transitions of smectic poly(ester imide)s by means of small-angle X-ray scattering

Received: 16 July 1999
Accepted: 28 April 2000

C. Wutz (✉) · N. Stribeck · D. Gieseler
Institut für Technische und
Makromolekulare Chemie
Universität Hamburg
Bundesstrasse 45, 20146 Hamburg
Germany

Abstract The molecular order and phase transitions of two smectic poly(ester imide)s based on aminobenzoic acid trimellitimide (PEI 1) or aminocinnamic acid trimellitimide (PEI 2) and α,ω-dihydroxydodecane were investigated by X-ray scattering. During cooling, the polymers pass through monotropic smectic liquid-crystalline (LC) phases (S_A, S_C), which transform into higher-ordered smectic-crystalline phases (S_E, S_H). The smectic layer structure of about 3 nm gives rise to a sharp reflection at $2\theta \cong 3°$. Peak shape analysis and analysis of the interface distribution function revealed long-range longitudinal correlation among the mesogens in the LC phase but short-range lateral correlation. The development of a broad reflection in the small-angle X-ray scattering (SAXS, $2\theta < 1°$) indicates the formation of a lamellar two-phase system. The long-period changes reversibly between 10 and 30 nm with increasing temperature. The crystalline lamellae comprise a number of smectic-crystalline layers with packed mesogens, while the noncrystalline interlamellar regions keep their smectic-LC order. In the metastable S_B phase, formed during annealing of quenched PEI 1, the diffuse SAXS indicates a random distribution of small, probably fringed, crystals with hexagonal-packed mesogens. In the lamellar S_E and S_H phases, tie molecules play an important role, but chain folding cannot be excluded.

Key words Smectic · Poly(ester imide)s · Small-angle X-ray scattering · Lamellar

Introduction

Polymers with a regular sequence of rigid, polar mesogens and flexible, nonpolar spacers in the main chain tend to form smectic layer structures. In recent years, a number of such smectic main-chain polymers have been synthesized and characterized by microscopy, differential scanning calorimetry (DSC) and X-ray scattering [1–10]. In addition to the smectic liquid-crystalline (LC) phases S_A and S_C, several so-called higher-ordered smectic phases exist, which are denoted as S_B, S_E, S_F, and S_H depending on the lateral order of the mesogens and their orientation with respect to the layer plane [11]. For convenience, the molecular order of the smectic mesophases is represented schematically in Fig. 1. While the fluctuations of the mesogens in the LC phase result in a halo in the wide-angle X-ray scattering (WAXS, 2θ = 8–40°), higher-ordered smectic-crystalline phases display sharper reflections owing to the regular packing of the mesogens. In contrast to a three-dimensional crystal, no positional order exists among the mesogens of adjacent layers owing to the conformational disorder of the spacers [12, 13]. In contrast to low-molar-mass compounds, the smectic-crystalline phases of polymers are solid, since the molecular chains pass through a number of layers and prevent them from slipping off. In any smectic phase the layer order gives rise to a sharp reflection in the middle-angle X-ray

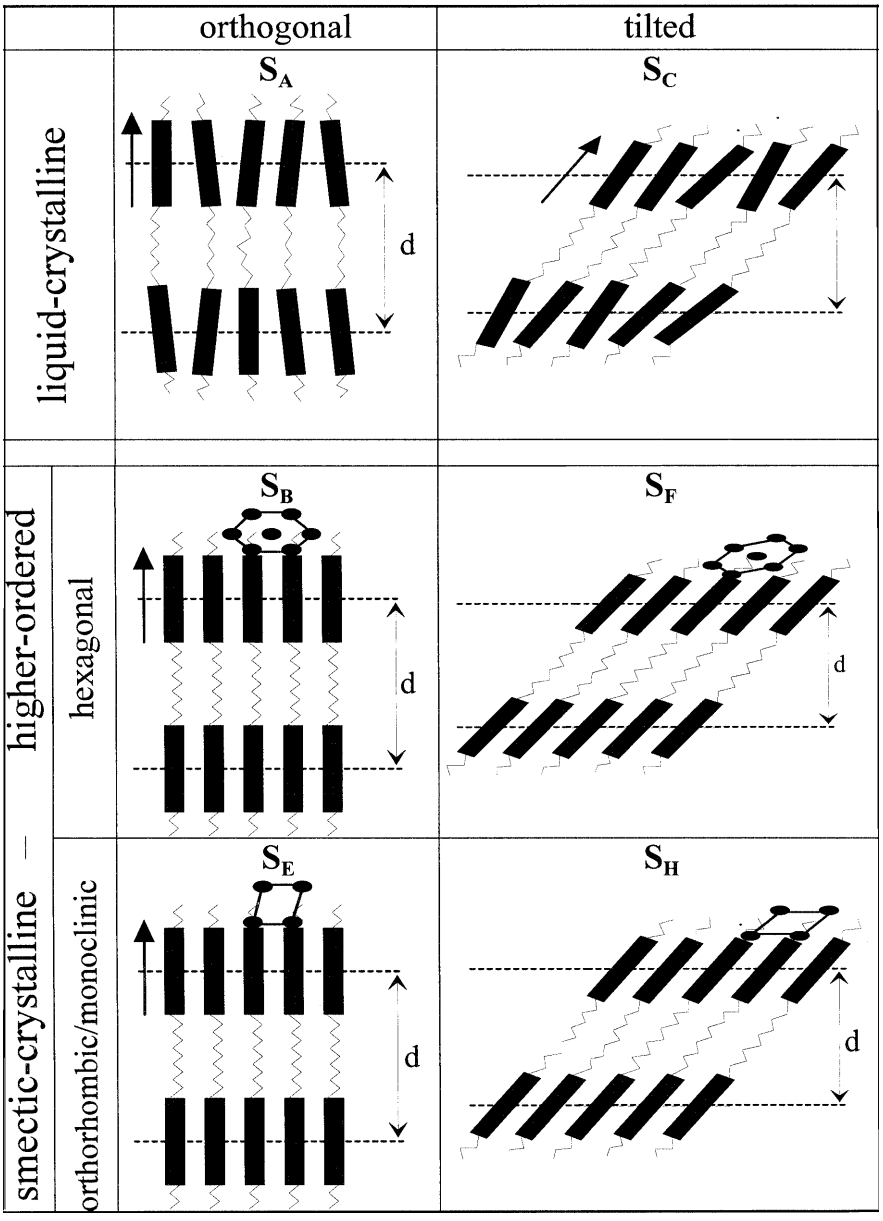

Fig. 1 Schematic representation of the molecular order in different smectic mesophases

scattering (MAXS, 2θ = 1–7°). Its position depends essentially on the length of the mesogen plus the spacer (d = 15–50 Å).

It has turned out that the poly(ester imide)s (PEI)1 and 2 depicted in Fig. 2, represent excellent model compounds for the investigation of the smectic layer order, because they form a variety of smectic phases dependent on the type mesogen, the spacer length, and the thermal treatment. The general phase behavior has been studied previously by polarization microscopy, DSC, time-resolved WAXS/MAXS measurements and X-ray fiber patterns [14–17]. Both PEI 1 and 2 display only monotropic, metastable LC phases during cooling. While the smectic phases of PEI 1 are exclusively orthogonal, the mesogens are tilted or staggered in PEI 2 [17]. The transition sequences of quenched PEI samples are listed as follows (temperatures determined by DSC 10 °C/min):

PEI 1 heating: $S_A(\text{glass}) \xrightarrow{80\,^\circ C} S_B \xrightarrow{120\,^\circ C} S_E \xrightarrow{170\,^\circ C} I$

cooling: $S_E \xleftarrow{115\,^\circ C} S_A \xleftarrow{135\,^\circ C} I$

PEI 2 heating: $S_C(\text{glass}) \xrightarrow{75\,^\circ C} S_H \xrightarrow{167\,^\circ C} I$

cooling: $S_H \xleftarrow{111\,^\circ C} S_C \xleftarrow{154\,^\circ C} I$

Generally, the temperature interval of the LC phase becomes narrower with increasing spacer length, so in the case of PEI 1 $n > 12$ no LC phase is formed at all.

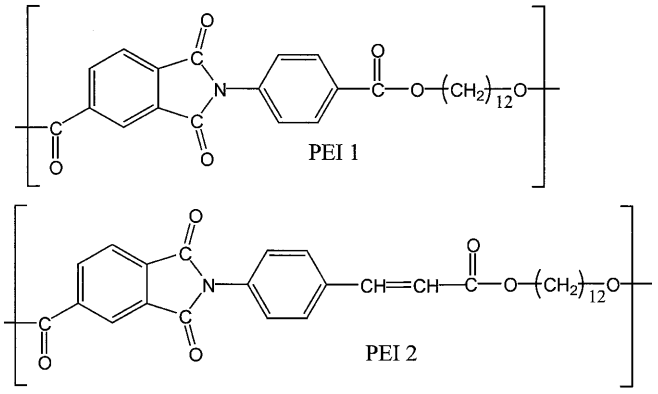

Fig. 2 Chemical structure of the poly(ester imide)s (PEI) 1 and 2

When the smectic-crystalline phase develops directly from the isotropic melt, none of the well-known LC textures are observed under the microscope, but a spherulitic morphology is observed [18, 19]. The particularity of these spherulites is their internal structure. They are constructed from "crystal" lamellae, each of them containing a number of smectic layers. The lamellar structure gives rise to a long-period reflection (150–300 Å) in the small-angle X-ray scattering (SAXS, $2\theta < 1°$). Our recent studies revealed that the smectic-crystalline phases, which develop from the LC phase, give rise to a SAXS peak as well. The scope of this work was to investigate the molecular order and the resulting SAXS of the smectic-crystalline phase and to provide deeper insight into the mechanism of crystallization from the smectic LC phase. In particular, it should be investigated to what extent the order of the mesogens in the smectic layers influences the crystallization process. Furthermore, we want to explore the potential of utilizing SAXS measurements for the classification and discrimination of smectic phases.

Experimental

Samples

The PEI were synthesized in the group of H.R. Kricheldorf and the syntheses and basic properties have been described elsewhere [14, 15], The polymers were molten at 200 °C in a hot press under vacuum for 2 min pressed into films of about 200-μm thickness, and quenched rapidly into ice–water. By this thermal treatment the LC phase is frozen in.

Measurements

The time-resolved X-ray scattering was measured using synchrotron radiation at the Hamburger Synchrotron Laboratorium Germany, at a wavelength of 0.15 nm with a one-dimensional detector and 30 s acquisition time per frame. The scattering curves were normalized with respect to the primary beam intensity, the background scattering was subtracted, and the curves were multiplied by s^2, with $s = (2/\lambda) \sin \theta$ being the scattering vector.

SAXS at ambient temperature was measured with a Kratky compact camera (Anton Paar). With an entrance slit height of 80 μm, an angular range of $s = 0.013$–1.1 nm was scanned. Ni-filtered Cu K_α radiation was employed. The scattering intensity was detected using a proportional detector. Calibration of absolute intensity was carried out using the moving slit device.

Peak shape analysis was carried out after a desmearing procedure using the Guinier–DuMond equation [20]. The method is presented in previous work [21]. The method of interface distribution function (IDF) analysis has been published previously as well [22, 23].

Results and discussion

Development of a lamellar system during the transition into the smectic-crystalline phase

The PEI samples were melt-pressed in the isotropic phase and quenched rapidly below the glass transition temperature (T_g). In this process crystallization is suppressed, but not the LC formation which has a much lower activation energy. The resulting films of the frozen smectic LC phase were studied by SAXS during the subsequent heating, cooling, and second heating cycle. As an example, Fig. 3 displays the development of the SAXS during first heating and cooling of PEI 2 at a rate of 10 °C/min. The first scattering curve reveals that the frozen smectic LC phase (S_C) exhibits no SAXS at all. The long-period reflection develops during the transition into the smectic-crystalline S_H phase above $T_g = 65$ °C. With increasing temperature, the reflection gains intensity and shifts towards smaller angles, until it vanishes completely in the isotropic melt (160 °C). Upon cooling, the sample passes through the LC phase between 155 and 130 °C and the SAXS develops once more during the transition into the S_H phase below 130 °C. It is important to note that the long-period reflection exhibits an unusual asymmetrical shape. The measurements on PEI 1 yielded similar results. Neither the frozen nor the liquid S_A phase passed during cooling displays SAXS. During first heating PEI 1 forms an intermediate, metastable S_B phase between 80 and 110 °C which does not show a SAXS peak, but which has weak diffuse scattering at very small angles. The long-period reflection arises during first heating above 110 °C or cooling below 120 °C with the transition into the smectic-crystalline S_E phase.

Tokita et al. [24] suggested that the SAXS reflection they observed from the crystalline phase of a main-chain polyester fiber results from chain foldings which may have already existed in the preceding LC phase. In our opinion it appears to be ambiguous, if a long-period reflection can arise exclusively from chain foldings at all, independent of being distributed randomly or concentrated at lamellar domain boundaries, since the volume of the disordered regions of lower electron density would be extremely small. Our results

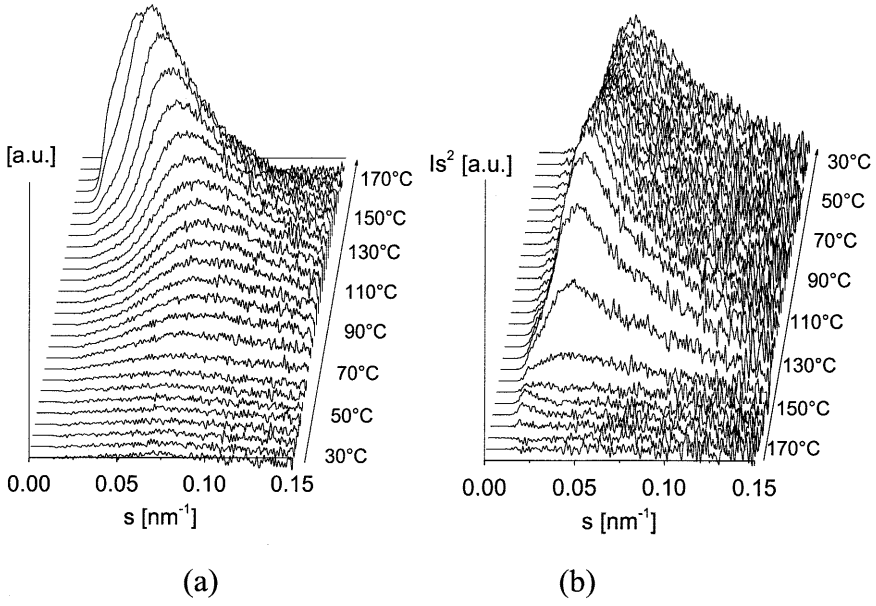

Fig. 3 Change in the small-angle X-ray scattering (SAXS) of PEI 2 during the first heating (**a**) and cooling (**b**) at 10 °C/min

agree with the observations of Tokita et al. [24] and Takahashi and Nagata [25] only in so far as the smectic LC phases display no SAXS.

Moreover, the occurrence of a SAXS reflection during the transition from the LC into the smectic-crystalline phase indicates the development of a two-phase system with a long period of 10–30 nm, which is most probably formed as a superstructure of the smectic layer order with a repeat period of about 3 nm. This morphology of solid smectic phases has also been observed by transmission electron microscopy and has been referred to as a "lamellar decoration" of the texture [26]. The required electron density difference results from the regular, crystal-like packing of the mesogens within the lamellae, in contrast to lighter packing in the less-ordered interlamellar regions. During the growth of the crystal lamellae, noncrystallizable material, like entanglements and chain ends, is rejected and segregated in the interlamellar regions.

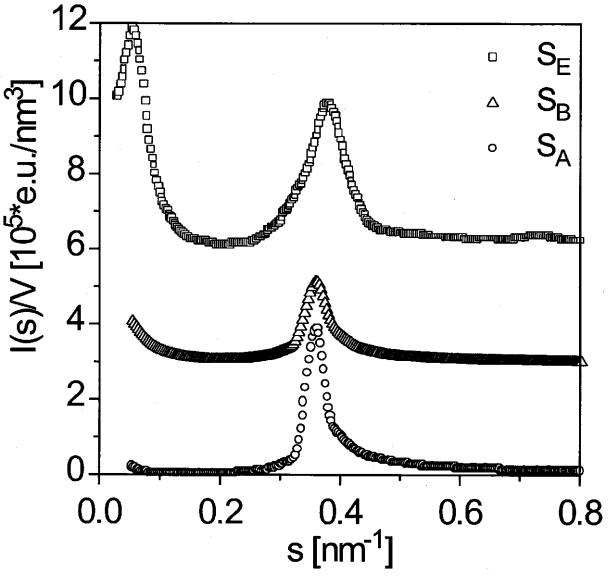

Fig. 4 SAXS MAXS curves of PEI 1 in the S_E (*top*), S_B (*middle*), and S_A (*bottom*) phases measured at ambient temperature with a Kratky camera

Molecular order in the different smectic mesophases

Before we discuss the transitions between the different mesophases, their molecular order as determined in more detail by the X-ray measurements is reported in the following. Three samples of PEI 1 with different mesophase structures were obtained by the following thermal treatment. All of them were melt-pressed in the isotropic phase and quenched rapidly. The first sample remained untreated and displayed a frozen S_A structure. The second and third samples were annealed at 90° and 135 °C, respectively, for 12 h to form the S_B and S_E phases, respectively.

The X-ray scattering curves of absolute electron density difference after slit-desmearing and background subtraction are depicted in Fig. 4. One can see the MAXS reflections of the smectic layer structures at 0.35 nm^{-1}, the long-period SAXS reflection of the S_E phase at 0.05 nm^{-1}, and the previously mentioned diffuse scattering at small angles of the S_B structure. The scattering curves exhibit the Porod law of a two-phase system. After subtraction of the density fluctuation background, the interference functions of ideal two-phase systems were determined. By Fourier–Bessel

transformation, we obtained the IDFs [23] for the smectic layer order of the three samples and for the lamellar system of the S_E phase. The theoretical background and the data treatment of this evaluation procedure have been described elsewhere [20–23]. The IDFs of the smectic layers of PEI 1 in the S_A, S_B, and S_E phases are shown in Fig. 5. The experimental curves were computed assuming a two-phase model with size distributions of the mesogen and spacer layer of different electron density. Some parameters of the layer structures evaluated during this analysis are collected in Table 1. The layer spacing, d_s, is represented by the first curve minimum. The correlation length, h_s, was evaluated via Scherrer's equation from the half width of the MAXS peaks (Fig. 4) and used as a parameter in the IDF fit.

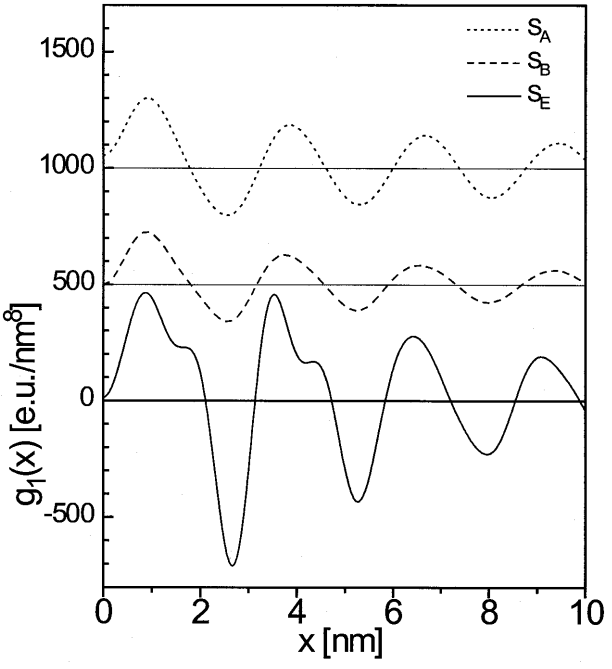

Fig. 5 Interface distribution functions calculated from MAXS data of the smectic structures of PEI 1 in the S_A (*top*), S_B (*middle*), and S_E (*bottom*) phases

Table 1 Average spacing of the smectic layers, d_s, electron density difference between the mesogen and the spacer layer, $\Delta\rho$, variation of the mesogen layer thickness, σ_m/d_m, and correlation length of the smectic system, h_s

	S_A	S_B	S_E
d_s (nm)	2.66 ± 0.04	2.62 ± 0.03	2.64 ± 0.02
$\Delta\rho$ (e.u./nm^3)	134 ± 4	114 ± 1	173 ± 5
σ_m/d_m	0.72 ± 0.03	0.57 ± 0.02	0.49 ± 0.02
h_s (nm)	27	20	9.5

All three smectic layer systems represent at least a one-dimensional lattice with a d spacing of $d_s = 2.65 \pm 0.05$ nm, which corresponds to the length of the chemical repeat unit. Previous studies demonstrated that the smectic layers are irregularly undulated in the LC phase and become flatly extended in the smectic-crystalline phase owing to the lateral packing of the mesogens [17].

As expected, the electron density difference between the mesogen and the spacer layer, $\Delta\rho$, increases from 134 e.u./nm^3 in the S_A phase to 173 e.u./nm^3 in the S_E phase and the variation of the mesogen layer thickness, σ_m/d_m, decreases owing to the lateral ordering of the mesogens during crystallization. In contrast, the correlation range, h_s, among the smectic layers diminishes; in other words, the variation of the d spacing increases. Since the mesogen layers are more uniform in the smectic-crystalline phase, the loss of long-range order has to be a result of a larger variation in the effective spacer lengths. This change in the spacer properties has been observed previously by the conformational analysis of the spacer segments of PEI 1 and 2 by ^{13}C solid-state NMR [12]. The length h_s evaluated from Scherrer's equation represents a lower limit of the correlation. The value of 27 nm for the S_A phase corresponds to ten repeat units. This result proves that the mesogen position along the chain exhibits an extremely high periodicity in the LC phase, in contrast to the poor lateral order. The resulting stacks of warped layers give rise to layer line-shaped MAXS reflections in the fiber pattern [17]. In the smectic-crystalline S_E phase, the value of $h_s = 9.5$ nm indicates that the correlation range in the chain direction is decreased but covers at least four smectic layers.

The IDF of the lamellar superstructure evaluated from the SAXS of the S_E phase is represented in Fig. 6.

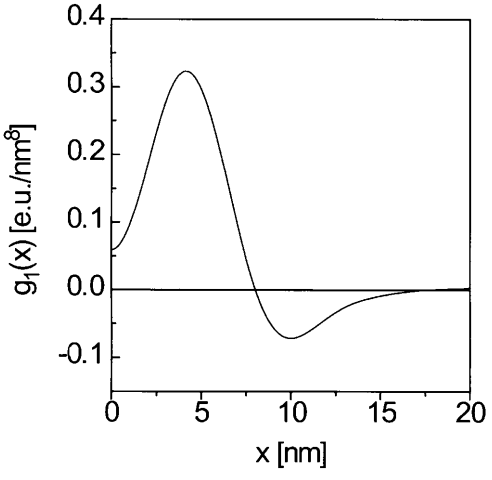

Fig. 6 Interface distribution function of the lamellar system of PEI 1 in the S_E phase calculated from SAXS data

In addition to the long period of $L = 10.2$ nm (curve minimum), the average thickness of the two phases is determined to be 4.6 and 5.6 nm, respectively. The 4.6-nm layer exhibits a symmetric, relatively narrow size distribution which is attributed to the ordered lamellae containing mainly double layers of crystalline mesogens. The broad and extremely asymmetric distribution around 5.6 nm corresponds to the noncrystalline interlamellar regions. A comparison with the previously mentioned MAXS correlation length of $h_s = 9.5$ nm indicates that the range of smectic layer order exceeds the height of the "crystalline" lamella; hence, we conclude that the noncrystalline interlamellar regions exhibit a residual metastable smectic-LC structure, as suggested in a model by Thomas and Wood [26]. Consequently, the variation of the mesogen layer thickness, $\sigma_m/d_m = 0.49$ (Table 1), represents an average value of the noncrystalline regions and the crystalline layers, which are certainly even more uniform. The structure and electron density distribution in the smectic-crystalline phase are illustrated schematically in Fig. 7. The complete, quantitative evaluation of the SAXS data and the derived detailed lattice model of the S_E phase is the subject of another publication [21].

The SAXS curves in Fig. 3 display the broad and asymmetrical shape of the long-period reflection, which indicates a disproportionate size distribution. The IDF in Fig. 6 reveals that the correlation length of the lamellar system barely exceeds the long period, so the structure cannot be classified properly as a lamellar stack. Since the thickness of the lamellae is relatively uniform, the weak correlation is the result of the broad, asymmetrical distribution of the noncrystalline, interlamellar regions. Our SAXS measurements from the S_E and S_H phases of PEI 1 and 2 thus reveal a substantial difference to the S_H phase of the main-chain polyester reported by Tokita et al. In the latter case, the periodicity of the lamellar system was particularly high, so second-order and even third-order reflections of the long period could be detected [27]. It should be mentioned, however, that the S_H phase of the polyester was obtained by crystallization from the isotropic phase, whereas the smectic-crystalline phases in the present study are formed out of the smectic LC phase. On the other hand, the SAXS investigations of PEI with longer spacers, which form smectic-crystalline phases with a spherulitic superstructure from the isotropic melt, exhibited the same broad, asymmetrical long-period reflection [18].

The asymmetrical size distribution of the noncrystalline regions could result from molecular tensions occurring during the crystallization process. This notion has been discussed by Dehlinger and Kochendörfer [28]. However, the molecular tensions in the PEI are not caused by the LC preorder as mentioned earlier. Moreover, they may be due to the long monomer length and the resulting coarse quantization of the lamella thickness. Asymmetry of the SAXS peak was also observed by Rueda et al. [29] in a semicrystalline poly(ether ketone) with a very long repeat unit. Whereas a polyethylene crystal of 5-nm thickness contains 20 monomers of 0.25 nm, the smectic crystalline lamellae of the PEI comprise only 2–3 repeat units. The average reptation length of a chain segment which is necessary to fit a mesogen into the crystal lamella is much longer. The reptation of the segment exerts stress upon the chain, if another mesogen of the same chain nearby is already part of another crystal. The characteristic properties of such tense crystals will be demonstrated later.

In the case of PEI based on trimellitic acid a particular difficulty occurs during this process because the mesogens have an asymmetrical chemical structure and their sequence with respect to the direction along the chain is probably random. These structural irregularities cause a minimum of disorder around the ordered lamellae.

Temperature dependence of the SAXS

In the following, studies of the temperature-dependent structural changes of PEI 1 and 2 using time-resolved SAXS measurements with synchrotron radiation are reported. As demonstrated in Fig. 3, the long-period reflection occurs during the transition into the smectic-crystalline state.

From the SAXS curves, the long-period, L, and the relative scattering power, Q, were evaluated using Eqs. (1) and (2)

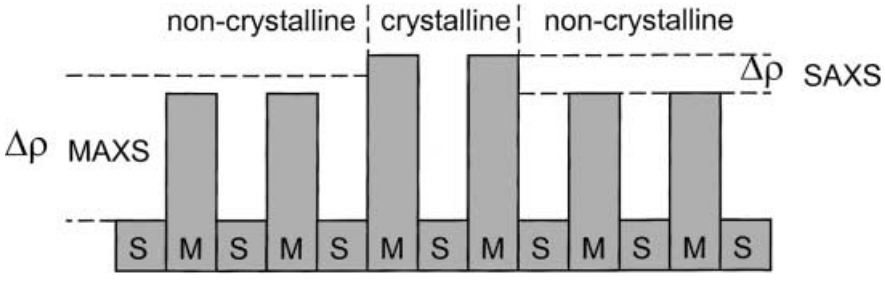

Fig. 7 Schematic representation of the electron density distribution in the ideal two-phase system of the smectic-crystalline phase. The mesogen and the spacer layers are represented by *M* and *S*, respectively

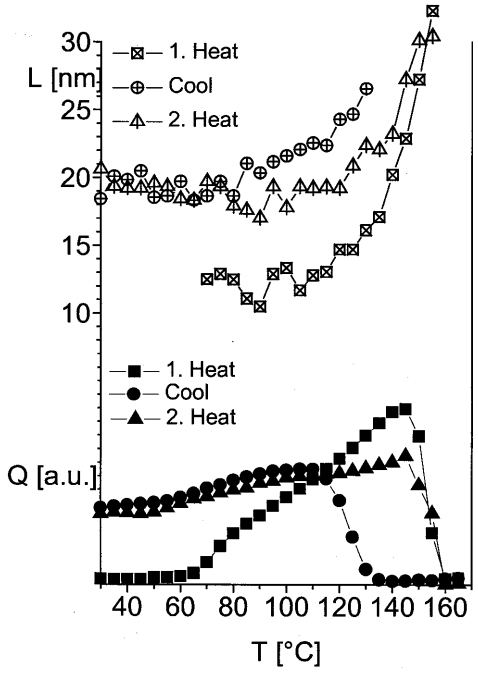

Fig. 8 Long period, L, and relative scattering power, Q, of quenched PEI 2 as a function of the temperature during first heating, cooling, and second heating

$$L = \frac{1}{s_{\max}} \quad , \tag{1}$$

$$Q = \int I(s)\, s^2\, \mathrm{d}s \quad . \tag{2}$$

Due to the asymmetry of the SAXS peak, the L values determined by Eq. (1) may differ slightly from the results of the IDF, but at least they demonstrate the temperature-dependent variations. As an example, Fig. 8 represents L and Q of quenched PEI 2 as a function of the temperature during a cycle of first heating, cooling, and second heating. During the crystallization from the glassy state, thin lamellae with a long period of about 10 nm are formed first. The substantial increase in L above 130 °C can be attributed to partial melting. The thinnest, most disturbed, or tensest crystals melt out of the lamellar system and the average d spacing is increased. Upon cooling, the sample passes through the monotropic LC state which displays no SAXS. Below 120 °C, the increase in Q indicates the transition into the smectic-crystalline phase. During this process, the long period decreases, as reported for the crystallization of conventional, semicrystalline polymers, because thick main lamellae grow at first, followed by the development of smaller crystals between them in a kind of secondary crystallization process. However, the final long period remains larger than for the crystallization from the glassy state, because the thickness of the lamellae increases with the crystallization temperature owing to the larger size of the critical nucleus and the improved molecular mobility. Both effects usually results in a higher degree of crystallization achieved at elevated temperatures. Figure 8 displays, however, that the scattering power, Q, obtained during crystallization from the melt is lower than the maximum Q value observed during first heating. This observation can be explained by Eq. (3), which relates Q to the fraction of the crystal lamellae, X_{CL}, the fraction of the interlamellar regions, 1-X_{CL}, and the electron density difference, $\Delta\rho$.

$$Q \propto X_{\mathrm{CL}}(1 - X_{\mathrm{CL}})\ \Delta\rho^2 \tag{3}$$

On the one hand, the fraction of lamellae formed during first heating amounts to approximately $X_{\mathrm{CL}} = 0.5$ (Table 1), resulting in a maximum Q value. During crystallization from the melt the lamellae are thicker as indicated by the long period in Fig. 8. If X_{CL} exceeds the value of 0.5 significantly, the scattering power becomes lower according to Eq. (3). On the other hand, our absolute SAXS measurements reveal that the electron density difference between the crystalline lamellae and the interlamellar regions, $\Delta\rho$, is larger for a S_E phase formed from the glassy state than for crystallization from the melt. We suggest that the molecular tensions are greater during crystallization from the glassy state owing to the restricted molecular mobility. They enforce a bigger overlap of the incompatible mesogens and spacers and their repulsion decreases the density of the noncrystalline phase. As a result, the electron density difference to the crystalline phase, $\Delta\rho$, and, according to Eq. (3), the scattering power are increased in comparison to the cyrstallization from the melt. During cooling below 110 °C and subsequent heating, Q changes reversibly owing to the different thermal expansion coefficients of the crystalline and the noncrystalline phases.

Since the smectic LC phases of PEI 1 and 2 are only metastable, the transition into the smectic-crystalline phase takes place under isothermal conditions as well. The development of the long period of PEI 1 during crystallization at different temperatures is shown in Fig. 9a. The decrease in the long period in the initial stage of the process proves that the assumption of the previously mentioned mechanism of main and subsidiary lamellae is also valid for isothermal conditions. The final long period is a function of the crystallization temperature (Fig. 9b) according to the Thomson–Gibbs equation and is in agreement with the observations of Tokita et al. [24].

Folded or fringed crystal?

For several decades, scientists have discussed whether a folded chain or a fringed micelle represents an adequate

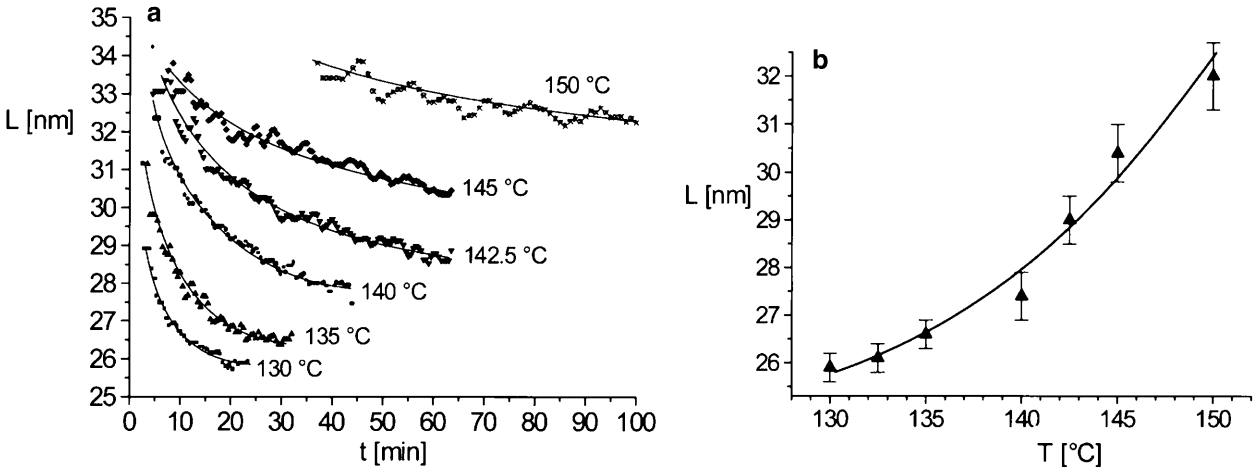

Fig. 9 **a** L as a function of time during isothermal crystallization of PEI 1 at different temperatures and **b** final L value as a function of the temperature

model for polymer crystals. Nowadays, it is generally accepted that the crystal lamellae of most semicrystalline polymers contain a considerable number of chain folds.

In contrast, crystallization from the nematic LC phase of random copolymers with stiff main chains is a good example for fringed crystal formation [30–32]. Owing to their poor lateral extension and their random spatial distribution they produce no long-period reflection but only a diffuse SAXS.

In segmented main-chain polymers the flexible spacers are readily long enough to accommodate folds, so the realization of both types of crystals is possible and the discrimination is frequently difficult [26]. Tokita et al. [24] suggested a folded lamellar system for the S_H phase of the main-chain polyester, on the basis of the unusual flow orientation of the polymer in the preceding LC phase. In the tense crystal system we propose the tie molecules between the lamellae, typical for fringed crystals, play an important role and the reported in the following investigations provide evidence of their existence.

The S_B phase of PEI 1 formed during annealing of the quenched sample exhibited only a diffuse SAXS as depicted in Fig. 4. In this behavior the S_B phase differs from the smectic LC phases (S_A, S_C), which exhibit no SAXS, and the lamellar smectic-crystalline phases (S_E, S_H), which give rise to a discrete SAXS. We conclude that the S_B phase contains a random distribution of small aggregates with hexagonal-packed mesogens. which give rise to the single WAXS reflections at $2\theta = 20.2°$ reported previously (Fig. 1B in Ref. [33]). Since these individual crystals are only metastable and develop exclusively from the frozen smectic LC phase with restricted chain mobility, a fringed molecular order can be assumed.

In the S_E and S_H phases of PEI 1 and 2, the lamellar structure gives rise to the SAXS peak as described earlier. This observation gives, however, no clear evidence for the existence of purely folded lamellae. In the folded crystals of conventional, semicrystalline polymers the chain folds at the lamella surface limit the thickening of the crystal. The commonly observed increase in the long period during annealing is due to the partial melting and recrystallization of thicker lamellae. This process is irreversible and the long period remains constant during subsequent cooling, as long as the sample was not completely molten. In this respect, the smectic-crystalline PEI exhibit a significantly different behavior. In Fig. 10 one can see that the SAXS reflection shifts towards larger angles upon cooling even after entire isothermal crystallization. We found that the long period measured at a certain temperature represents an equilibrium value independent of the thermal pretreatment. This observation may be interpreted as a characteristic mesophase behavior; the reason is, however, not quite clear. Either addi-

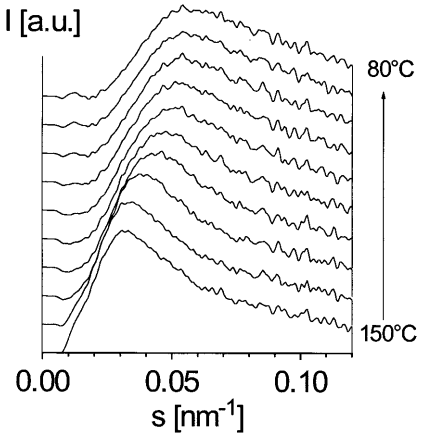

Fig. 10 Change in the SAXS of PEI 2 during cooling at 10 °C/min after entire isothermal crystallization at 150 °C

tional crystals are formed within the interlamellar regions during cooling, owing to the increasing enthalpic interactions among the mesogens or an increasing number of thinner lamellae are formed at the expense of a few thick lamellae. Since the integral intensity of the crystal WAXS reflections remains virtually constant during this process, the second mechanism is more likely. The observed reversible changes of the lamellar structure can be explained more easily by assuming a fringed micelle system, because in a chain-folded crystal system they would require long-range chain reptations. Anyway, this effect is clearly not a result of the orientational order of the preceding LC phase, because it is also observed for those PEI which form the smectic-crystalline phase directly from the isotropic melt (Fig. 11 in Ref. [18]). Obviously, the temperature-dependent reversible changes of the lamellar structure are typical for the smectic-crystalline phase independent of the mechanism of its formation.

Although the present results do not allow a clear discrimination between folded and fringed crystals, it can be assumed that the tensions among the crystal lamallae are exerted by tie molecules, while they are reduced by chain folds. Consequently, it can be speculated that the crystals formed from the frozen LC state represent fringed micelles, while chain folds have to be considered for the crystallization from fluid phases.

Conclusions

The X-ray scattering results of the present study reveal that during the transition from smectic LC (S_A, S_C) to higher-ordered smectic phases (S_E, S_H) of the PEI a lamellar two-phase system is formed. Each crystal lamella comprises a number of smectic layers with regularly packed mesogens. The interlamellar regions are unable to crystallize owing to the random sequence of asymmetrical mesogens and the concentration of entanglements and chain ends, and form a residual smectic LC phase. The reversible, temperature-dependent changes of the lamellar structure indicate the mesophase character of the smectic-crystalline phase. The present SAXS measurements give no clear evidence of whether a chain-folded or a fringed crystal represents suitable model for the smectic-crystalline lamallae. The hexagonal S_B phase of PEI 1 formed from the smectic glass is assumed to consist of individual fringed crystals.

Acknowledgement The authors are grateful to H.R. Kricheldorf for providing the PEI samples.

References

1. Ober CK, Jin JI, Lenz RW (1984) Adv Polym Sci 59:103
2. Watanabe J, Hayashi M, Nakata Y, Niori T, Tokita M (1997) Prog Polym Sci 22:1053
3. Blumstein A, Vilasagar S, Ponrathnam S, Clough SB, Blumstein RB (1982) J Polym Sci Part B Polym Phys 20:877
4. Pardey R, Zhang A, Gabori PA, Harris FW, Cheng SZD, Adduci J, Facinelli JV, Lenz RW (1992) Macromolecules 25:5060
5. Yoon Y, Ho R, Moon B, Kim D, McCreight KW, Li F, Harris FW, Cheng SZD, Percec V, Chu P (1996) Macromolecules 29:3421
6. Francescangeli O, Yang B, Laus M, Angeloni AS, Galli G, Chiellini E (1995) J Polym Sci Part B Polym Phys 33:699
7. Kricheldorf HR, Linzer V (1995) Polymer 36:1893
8. Kricheldorf HR, Probst N, Schwarz G, Wutz C (1996) Macromolecules 29:4234
9. Wutz C, Thomsen S, Schwarz G, Kricheldorf HR (1997) Macromolecules 30:6127
10. Schwarz G, Thomsen S, Wutz C, Bartos S, Kricheldorf HR (1998) Acta Polym 49:173
11. Gray GW, Goodby WG (1984) Smectic liquid crystals. Hill, New York
12. Wutz C, Schleyer D (1998) J Polym Sci Part B Polym Phys 36:2033
13. Cheng J, Yoon Y, Ho R-M, Leland M, Guo M, Cheng SZD, Chu P, Percec V (1997) Macromolecules 30:4688
14. Kricheldorf HR, Schwarz G, de Abajo J, de la Campa J (1991) Polymer 32:942
15. Kricheldorf HR, Probst N, Wutz C (1995) Macromolecules 28:7990
16. Wutz C (1997) Mol Cryst Liq Cryst 307:175
17. Wutz C, Gieseler D, Maevis T, Stribeck N (1999) Macromolecules 32:4658
18. Wutz C (1988) Polymer 39:1
19. Wutz C, Schäfer R (1999) Mol Cryst Liq Cryst 326:75
20. DuMond JWM (1947) Phys Rev 72:83
21. Stribeck N, Wutz C (2000) J Polym Sci Part B Polym Phys (accepted)
22. Ruland W (1977) Colloid Polym Sci 255:417
23. Stribeck N (1993) Colloid Polym Sci 271:1007
24. Tokita M, Takahashi T, Hayashi M, Inomata K, Watanabe J (1996) Macromolecules 29:1345
25. Takahashi T, Nagata FJ (1989) Macromol Sci Phys B 28:349
26. Thomas EL, Wood BA (1985) Faraday Discuss Chem Soc 79:229
27. Tokita M, Osada K, Yamada M, Watanabe J (1988) Macromolecules 31:8590
28. Dehlinger U, Kochendörfer AZ (1939) Z Kristallogr 101:134
29. Rueda DR, Garcia Gutierrez MC, Ania F, Zolotukhin MG, Balta Calleja FJ (1998) Macromolecules 31:8201
30. Hanna S, Windle AH (1988) Polymer 29:207
31. Biswas AJ (1992) J Polym Sci Part B Polym Phys 30:1375
32. Plummer CJG, Kausch H-H (1997) Polymer 38:1745
33. Probst N, Wutz C, Kricheldorf HR (1998) Polymer 39:5535